

1 The behavior of the F_2 peak ionosphere over the South Pacific during quiet
2 summer conditions from COSMIC data.

3

4

5 A. G. Burns, Z. Zeng, W. Wang, J. Lei, S. C. Solomon, A. D. Richmond, T. L. Killeen, C.
6 Rocken and Y.-H. Kuo.

7

8

9 For submission to J. Geophys. Res., 2008

1 **Abstract.**

2

3 The six satellite Constellation Observing System for Meteorology, Ionosphere and
4 Climate (COSMIC) mission makes routine ionospheric measurements over the entire
5 globe using occultation techniques. These observations have been used in this study to
6 develop global-scale climate maps of NmF_2 and hmf_2 during the southern (northern)
7 summer (winter). The southern, Equatorial (Appleton) anomaly becomes displaced
8 southward at dusk and, within about an hour, appears to form the Weddell Sea anomaly.
9 Coincidentally, the height of the F_2 peak increases on the northernmost boundary of the
10 anomaly. This height increase is also displaced southward as the anomaly is displaced
11 southward, suggesting that the electron density increases are associated with the F_2 peak
12 rising. As well as being an interesting phenomenon in its own right, this behavior may
13 also sheds new light on the formation of the Weddell Sea anomaly. No explanation for
14 this behavior can be determined from the data presently available, although several
15 mechanisms can be eliminated.

16

1 **Introduction.**

2

3 The Constellation Observing System for Meteorology, Ionosphere, and Climate
4 (COSMIC) mission consists of six satellites that measure, amongst other things, GPS
5 occultations. This measurement involves calculating the along-track differential phase
6 delay from a signal sent by the GPS satellites (*Rocken et al., 2000; Lei et al., 2007*) as it
7 is travels through the Earth's ionosphere and atmosphere near the horizon. The electron
8 density at the tangent point can be calculated from this phase delay. Maps of variations in
9 electron density have been built up for this paper using these data.

10 Some earlier published studies showed that the climatology obtained from COSMIC
11 ionospheric data (*Lei et al., 2007*) behaved in a way that was similar to both ionosonde
12 data and the IRI model (e.g., *Bilitza et al. 2007*) in magnitude and morphology. Other
13 features that were also seen by Lei et al. included well-known ionospheric phenomena.
14 For example, they saw the north-south asymmetry of the Equatorial anomalies and
15 variations in their longitudinal structure.

16 A recent example of the behavior that can be deduced from these observations was given
17 in a paper by *Zeng et al. (2008)*. They used the COSMIC data to study the nature and
18 causes of the annual anomaly in F_2 peak electron densities and found that the National
19 Center for Atmospheric Research- thermosphere-ionosphere-electrodynamics general
20 circulation model (NCAR-TIEGCM) reproduced the COSMIC observations very well.
21 They also found that the annual anomaly in electron density was primarily driven by the
22 geometry of the Earth's magnetic field, but that the changing Sun-Earth distance did play

1 a role as well. These studies show that COSMIC data is suitable for climatological
2 studies of the ionosphere during quiet conditions.

3 Before describing the feature that is the center point of this paper it is worth describing
4 the main features of the F_2 peak climatology (e.g., see *Rishbeth and Garriott, 1969*). The
5 dominant F_2 peak ion is O^+ . This ion is primarily produced by the photoionization of O
6 and it is lost through recombination with the neutral gases O_2 and N_2 . As these gases are
7 heavy, their densities decrease rapidly with height so the topside ionosphere reaches an
8 quasi-equilibrium state as a result of ambipolar diffusion (e.g., *Jee et al., 2006*). Other
9 transport processes are also important, particular the ion drifts that are driven by ExB
10 forcing near the magnetic equator.

11 A simple ionospheric pattern would occur if the horizontal structure of the neutral gases
12 was uniform and the transport processes were not important: the F_2 peak ionosphere
13 would have a circular pattern in which the electron densities decreased horizontally away
14 from the subsolar point. This pattern is very similar to the pattern of electron densities
15 that does exist in the F_1 region.

16 In the actual ionosphere transport processes and variations in neutral composition and
17 temperature cause anomalies. The most famous of these anomalies are the equatorial or
18 Appleton anomalies (e.g., *Rishbeth and Garriott, 1969*), which are two bands of
19 enhanced electron densities that lie parallel to the magnetic equator and are centered at a
20 geomagnetic latitude of about 20 degrees. They are prominent in the daytime and extend
21 for a long time into the night. They are driven by the electric field at the magnetic equator
22 and the subsequent redistribution of electron density.

1 Another well-known feature of the ionosphere is the winter anomaly (e.g., *Rishbeth and*
2 *Garriott, 1969*). In this anomaly the daytime electron densities are greater in the winter at
3 middle latitudes than they are in the summer. This anomaly is caused by the distribution
4 of neutral composition. O densities are large in winter and relatively small in summer,
5 whereas the molecular species have the opposite morphology. The balance between
6 production and loss then causes the higher electron densities in winter.

7 There is another anomaly in the climatological behavior of F_2 electron density which has
8 been far less studied, but which was also been known for 50 years. This is the Weddell
9 Sea anomaly (e.g., *Bellchambers and Piggott, 1958; Horvath, 2006*).

10 The Weddell Sea anomaly was discovered as a result of a large number of ionospheric
11 observatories being placed in Antarctica during the International Geophysical year in
12 1957. These data were analyzed by a number of researchers (e.g., *Bellchambers and*
13 *Piggott, 1958; Penndorf, 1965; and Dudeney and Piggott, 1978*), who noticed that a
14 peculiar phenomenon occurred in the electron densities at the F_2 peak over the Weddell
15 Sea region of Antarctica. They found that, in summer, electron densities were larger at
16 night than during the daytime. No such anomaly occurred in this region in winter. A
17 number of papers were written describing and attempting to explain this phenomenon.
18 Explanations include transportation from the dayside by the ion convection pattern
19 (*Penndorf, 1965*) and by neutral winds (*Dudeney and Piggott, 1978*). Both mechanisms
20 have issues. The former is problematic because, although the Weddell Sea is at high
21 geographic latitudes, it is in the middle latitudes geomagnetically. Ion drifts are
22 constrained by magnetic field lines and cannot readily transport plasma into the
23 geomagnetic middle latitudes. The latter also has problems as the nighttime enhancement

1 in the Weddell Sea anomaly always begins at dusk. The neutral winds that blow across
2 the magnetic polar cap in an antisunward direction have a jet near midnight. They flow
3 towards the Sun in the dusk region (e.g., see *Killeen and Roble, 1987*) and so this jet
4 cannot produce the Weddell Sea anomaly. An alternative forcing mechanism may involve
5 the day-to-night, solar EUV driven winds. This forcing mechanism could come into
6 effect because the Weddell Sea region is normally separated from the high latitude
7 convection pattern. For this mechanism to work, equatorward winds have to blow
8 electrons up field lines into regions of less recombination. However, winds are mainly
9 zonal at dusk (*Burns et al., 1995*) and so this mechanism should also not contribute to
10 increasing electron densities.

11 Possible explanations involving neutral composition were dismissed by *Bellchambers*
12 *and Piggott (1958)*. We also do not see any reason why there might be large neutral
13 compositional variations in this region. Later we discuss why the current data from
14 COSMIC is not compatible with an explanation involving neutral composition.

15 In general, there seems to be no explanation at present for this anomaly. We will show
16 later that this behavior is even more unusual than expected.

17 Recent work has been done by *Horvath (2006)* to categorize the Weddell Sea anomaly
18 using satellite data. Horvath used TOPEX/Poseidon data and gave a more complete
19 morphology of the Weddell Sea anomaly than has hitherto been available, as much of the
20 disturbance occurs over oceans from which ground based observations are not available.

21 This work showed that the anomaly is a large (~22 million square kilometers) feature that
22 extends between 60 and 160° W longitude and peaks between 50 and 60° S latitude.

1 The purpose of this paper is to present the evidence for anomalous behavior of the F_2
2 electron densities in the low and middle latitudes of the South Pacific Ocean just after
3 dark that leads to the formation of both the Weddell Sea anomaly and its extension across
4 the aforementioned Ocean. Although we attempt to narrow down the possible causes of
5 this behavior, there is insufficient evidence to provide a mechanism for its formation. The
6 paper is organized in the following way. The next Section briefly describes the COSMIC
7 data and the analysis of this data needed to obtain the seasonal climatology. Section 3
8 describes the observations, section 4 discusses these results and the final section is a
9 conclusion section.

10

11

12 **The Data**

13

14

15 Six satellites, called the Constellation Observing System for Meteorology, Ionosphere,
16 and Climate (COSMIC or FORMOSAT-3), were launched on April 15, 2006 (*Kumar,*
17 2006). Three different instruments make up their science payload. The instrument that
18 interests us here is the advanced GPS receiver. It is used to make the atmosphere and
19 ionosphere measurements through phase and Doppler shifts of radio signals. The Doppler
20 shift is used to compute the amount of signal bending that occurs as the impact parameter
21 varies (*Rocken et al., 2000*). This bending is then used to compute vertical profiles of
22 refractivity. The refractivity is directly proportional to ionospheric electron densities
23 when impact parameters are above 80 km (*Lei et al., 2007*). The Abel inversion technique

1 is then applied to retrieve electron density profiles from the total electron content along
2 these ray paths (*Hajj and Romans, 1998; Schreiner et al., 1999*).

3 The satellites were launched from the same rocket and initially followed the same orbit
4 track at 512 km. The satellites were then sequentially raised to orbits at 800 km. The time
5 delay for this increase in elevation has been designed to spread the orbital planes, so the
6 individual satellites are now 30 degrees apart. At this time the COSMIC satellites provide
7 approximately 24 hours of local time coverage globally and provide about 2500 vertical
8 electron density profiles per day. This distribution the global ionospheric measurements
9 by the COSMIC satellites provides an opportunity to investigate global ionospheric
10 structures and their variations. The data used here come primarily from the period when
11 the satellites were being maneuvered into this orbital configuration. Despite some lack of
12 coverage from this intermediate configuration, local time, universal time, longitude and
13 latitude coverage is mostly complete (see Figure 3). In the odd case where it is not, the
14 data are interpolated using the methodology described in the subsequent paragraph.

15 The data used in this study were retrieved from the COSMIC
16 (<http://www.cosmic.ucar.edu>) observations from launch until the August 2007. Disturbed
17 conditions with a k_p index larger than 3 were removed during this solar minimum period.
18 Abel inverted data (*Lei et al., 2007*) were used in this study to obtain values for NmF_2
19 and hmF_2 . The data were binned in a uniform horizontal grid with a resolution of 10° in
20 geographic longitude and 5° in geomagnetic latitude. For each subset, the data are sorted
21 in local time (LT) and a weighted average was applied (*Beers et al., 1990*) with a 2 hour
22 sliding window and a 1 hour moving step. The data were then separated into 91 day
23 seasons centered on the solstices and the equinoxes. Finally, a 7th order polynomial fitting

1 was applied to the averaged data to remove any data gaps in the local time domain (Zeng
2 *et al.*, 2008).

3

4

5 **Results**

6

7

8 Figure 1 gives global maps of NmF_2 calculated from COSMIC data for 4 local time bands
9 from 1700 local time to 2100 local time. Figure 1a gives this map for the 1700-1800 local
10 time band. This pattern is typical of the one described by *Lei et al.* (2007). An equatorial
11 anomaly is seen on both sides of the magnetic equator. The one in the northern (winter)
12 hemisphere is weaker than the one in the southern (summer) hemisphere. Longitudinal
13 structure is seen in these equatorial anomalies. The largest peak in the southern anomaly
14 is over South America, with possible secondary peaks over the Indian and Pacific Oceans.
15 The distribution of electron density in the northern equatorial anomaly appears more
16 uniform, but this is partially a function of the wide range of electron densities that the
17 green color represents. Apart from this, electron densities fall off towards higher latitudes,
18 with the smallest values of NmF_2 being found in the high latitudes of the northern, winter
19 hemisphere. There is some longitudinal structure at higher latitudes. For example, NmF_2
20 at 50° N maximizes over the Atlantic coast of North America.

21 The first deviation from this pattern is seen in Figure 1b, which shows values of NmF_2 in
22 the 1800-1900 local time band. There is an increase in electron density in the middle
23 latitudes west of South America which appears to be associated with the southern

1 Equatorial anomaly. Apart from this difference, the pattern is similar to that at the
2 previous local time, albeit with reduced values of NmF_2 globally. Maximum values of
3 NmF_2 occur in the southern equatorial over South America. Electron densities in the
4 southern equatorial anomaly are larger than those in the north and there is some
5 longitudinal structure in the anomalies. Longitudinally, electron densities in the middle
6 latitudes also vary much as they did at 1700 local time, except for the aforementioned
7 change that occurs over the South Pacific off Chile.

8 A much greater change occurs in the 1900-2000 local time band (Figure 1c). The summer
9 equatorial anomaly is displaced far south over the Pacific Ocean west of Chile; its center
10 is now between 45 and 60° S. The longitude region in which this occurs is fairly narrow,
11 stretching only from about 100 to 140° W for the southernmost excursion. The shape of
12 this excursion and its limited longitude range suggests a strong connection with the
13 extension of the magnetic equator into the southern hemisphere. There appears to be
14 continuity with the southern equatorial anomaly in this southern excursion, insofar as the
15 anomaly appears to have been displaced southward in a band from north of New Zealand
16 all the way to its southernmost location. Some of this may be inherent in the smoothing
17 used in the analysis procedure (however, Figure 3 suggests otherwise), but the quite wide
18 longitudinal extent of the excursions of the equatorial anomaly across the Pacific Ocean
19 suggests continuity in the processes that are leading to the excursion. Elsewhere in the
20 world the equatorial anomalies continue to behave in much the same way as they did at
21 earlier local times. The northern equatorial anomaly shows no changes in latitude; it just
22 gets weaker as was the case in the earlier Figure. The southern equatorial anomaly over
23 South America, the Atlantic and Indian Oceans also gets weaker but its latitude does not

1 change. There are still significant longitudinal structures in the anomalies in these
2 locations. Maxima are seen in the southern anomaly over South America, the west coast
3 of Africa and Indonesia. The northern equatorial anomaly has a peak over South America,
4 but other structure is difficult to discern.

5 The southern Pacific band of enhanced electrons is far south of its normal position in the
6 2000-2100 local time band (Figure 1d). The center of the enhanced electron densities is at
7 60° S in the Pacific Ocean west of Chile. The longitude of these enhancements is, in part,
8 west of the normal location of the Weddell Sea anomaly, although the region of enhanced
9 electrons does extend halfway across the Weddell Sea. A similar plot for the post
10 midnight period, which is not presented in this paper, shows that this region of
11 enhancements moves eastward through the night so that it covers the Weddell Sea region.
12 The existence of this region of enhancements over the Bellingshausen and part of the
13 Amundsen Sea soon after dusk does not indicate that they should have been observed by
14 ground stations. The enhanced densities exist over water, where TOPEX observations
15 have provided evidence of the Weddell Sea anomaly (*Horvath, 2006*). These TOPEX
16 observations show that the Weddell Sea anomaly extends into the South Pacific as far as
17 160° W, which is commensurate with the geographical distribution shown in this paper.

18 The disturbed area also extends further across the South Pacific, albeit at lower latitudes.
19 Electron densities are enhanced at middle latitudes over New Zealand. These
20 enhancements appear to connect continuously with the region of enhanced densities at
21 60° S and 140° W. An ionosonde in northern New Zealand should observe a slower
22 decrease in electron densities in the evening hours in summer than that which is seen at
23 equivalent middle latitude stations at other locations (e.g., Camden, Australia). Elsewhere

1 on the globe electron densities appear to be behaving as they did at earlier local times,
2 although the magnitude of NmF_2 is lower. The maximum in NmF_2 in the southern
3 anomaly has decreased considerably, leaving the peak over the West African coast as the
4 largest one in the southern equatorial anomaly. There is another peak in the southern
5 anomaly over Indonesia. The northern anomaly has diminished even more than the
6 southern anomaly in this local time band. It does still have something of the same
7 longitudinal structure as there are possible peaks over the West African coast and over
8 India.

9 The behavior of NmF_2 described above, has a counterpart in the behavior of hmF_2 , which
10 may shed some light on the mechanism driving the changes. Figure 2 gives four plots of
11 hmF_2 in bands from 1700-1800 local time to 2000-2100 local time. The first local time
12 band, from 1700-1800 local time, is shown in Figure 2a. The highest hmF_2 values occur
13 close to the magnetic equator, but not entirely coincident to it (see *Lei et al.*, 2007 for
14 possible reasons for this difference). The peak altitude is south of the magnetic equator
15 from Africa all the way eastward across most of the Pacific Ocean. It is north of the
16 magnetic equator over Brazil.

17 The height of the F_2 peak decreases significantly as latitudes increase away from the
18 magnetic equator. Lowest F_2 peak heights occur in a band in the northern hemisphere that
19 is just poleward of the northern equatorial anomaly. Here peak heights can be as low as
20 about 200 km; over 150 km lower than the greatest peak heights at the magnetic equator.

21 There are considerable variations in hmF_2 in the southern middle latitudes. Peak heights
22 occur at altitudes of between about 250 km and 280 km over the South Pacific, whereas
23 their altitude range is from about 230 to 250 km over the Indian Ocean. The values over

1 the South Pacific are our main concern in this paper, so these will be discussed more
2 completely in the subsequent paragraphs than those at other locations.

3 Figure 2b is a map of hmF_2 for the 1800 to 1900 local time band. Generally, hmF_2 is
4 occurring at higher altitudes over the whole globe at this time. The pattern is very similar
5 to that in the previous local time band over most of the globe. Highest values occur near
6 the magnetic equator and lowest values occur in the northern middle latitudes just
7 poleward of the northern equatorial anomaly. Of particular interest here is what happens
8 in the South Pacific. Increases in hmF_2 of the order of 20 to 30 km occur in this region,
9 with a distinct tongue shape westward of the center of the enhancements of NmF_2 .

10 The trends seen in the 1800 to 1900 local time band continue through into the 1900 –
11 2000 local time band (Figure 2c) Peak heights reach 300 -310 km as far south as 50° S in
12 the South pacific at about 120° W longitude. This represents an increase in altitude for
13 the peak height of at least 50 km on the northern edge of the region of enhanced electron
14 densities. The height increases are much smaller elsewhere in the southern middle
15 latitudes, indicating that this increase in F_2 heights in the South Pacific is part of the
16 process that drives the displacement of the southern equatorial anomaly in this region.

17 The last hmF_2 plot shows that, for 2000 to 2100 local time (Figure 2d), the height
18 increases in the South Pacific are even more dramatic. F_2 peak heights are above 325 km
19 at latitudes as high as 30 S in the South Pacific and about 315 km at latitudes as high as
20 45 degrees. Peak heights thus increase by 60 to 70 km in the middle latitudes of this
21 longitude sector. Increases in peak height are only about 30 km over middle latitude
22 locations in other parts of the Earth.

1 An obvious concern is that these changes in electron density that are observed over the
2 South Pacific, Bellinghausen Sea and Weddell Sea are merely the result of the analysis
3 procedures that were used. To counter this possibility we have looked at rawer forms of
4 the data. Figure 3 presents the data in the 2000 to 2100 local time bin as dots. The
5 location of these dots is determined by the position of the tangent point of the observation
6 as it goes through the F_2 peak. Although these data have been inverted using the Abel
7 inversion, no further analysis has been done on them. It can be seen that both the
8 magnitudes of NmF_2 and the pattern in which high electron densities are found over the
9 South Pacific Ocean occur in these data in much the same way as they do in the more
10 highly analyzed data shown in the earlier Figures. In other words, the post processing of
11 the observations did not change their main features, so the observed behavior is not just
12 an artifact of the processing used.

13

14

15 **Discussion**

16

17

18 The first question that arises when an unexpected phenomenon is seen in a data set is
19 whether or not the observations reflect what is really happening. Typically it is
20 impossible to absolutely prove that something is real, but a preponderance of evidence
21 can be amassed to indicate that it is probably happening.

22 We have tried to amass such a preponderance of evidence in this paper to indicate that the
23 dusk southward displacement of the southern equatorial anomaly in summer is a real

1 phenomenon. There are several aspects to this process. The first is to determine whether
2 the data set used reproduces other known phenomena. In this case the COSMIC data
3 produces many features that are also seen in other data sets. Prior to the southward
4 excursion of the southern equatorial anomalies, both sets of anomalies are located where
5 they are expected to be in relationship to the magnetic equator. There is the expected
6 seasonal variation in the magnitude and height of these anomalies and they exhibit
7 longitudinal variations that have been seen in other data sets.

8 There is no evidence in any other published work that we know of that the equatorial
9 anomaly can be displaced poleward to this extent. However, the end result of this
10 displacement is to produce an anomaly that involves electron densities at the F_2 peak over
11 the coast of Antarctica being larger at night than they are in the day in summer. This
12 anomaly was first reported by *Bellchambers and Piggott* (1958), who used ionosonde
13 measurements. It has also been measured by *Horvath* (2006) using TOPEX
14 measurements. In other words, it has been observed using more than one technique and is
15 an established phenomenon.

16 Given this, why would a synoptic feature as large as the displacement of the equatorial
17 anomaly over the South Pacific Ocean not have been discussed previously in the
18 literature? The answer may lie in its location over a region of the Earth that cannot be
19 observed from ground based stations. Before the comprehensive satellite measurements
20 from COSMIC became available, ionospheric observations over this region were limited
21 to difficult analyses of along track measurements by one satellite. Even with satellite
22 measurements it has not proved easy separate local time and longitude effects in electron

1 density measurements. The comprehensive set of COSMIC observations has changed this
2 situation.

3 Even though the phenomenon seen here appears to be supported indirectly by previous
4 studies, there is still a concern that the analysis procedures may introduce a false signal.

5 The need to isolate local time, latitude, longitude and universal time effects means that
6 there is considerable postprocessing of that data. For that reason we have presented the
7 data in a much rawer form to show that this postprocessing has not changed the pattern
8 significantly from that obtained by plotting out the individual measurements.

9 Thus, if the phenomenon described in this paper was an artifact of the data or the analysis
10 technique used then the COSMIC observations would have to be correct everywhere on
11 the globe except over the South Pacific. The coincidence of the enhanced COSMIC NmF_2
12 with the Weddell Sea anomaly would also have to be a chance correlation between a well
13 known phenomenon and some erratic data. Such coincidences would seem to be too
14 much to expect.

15 A difficult question arises if it is assumed that the phenomenon is real: what is causing it?
16 The data do provide some indications of what might be causing the displacement. The
17 lifting up of the F_2 peak on the equatorward side of this anomaly would involve ions
18 moving to heights where recombination was significantly decreased, leading to enhanced
19 electron densities. Ambipolar diffusion would tend to shift this enhanced ionization
20 downwards and polewards. Once the disturbance has reached the Weddell Sea anomaly
21 region it is illuminated even at night so some ionization can occur and electron densities
22 will remain large. In addition, the COSMIC data show that the F_2 peak is higher in the

1 Weddell Sea anomaly throughout the night (not plotted in this paper), which should mean
2 that loss rates are much diminished, allowing the Weddell Sea anomaly to persist.

3 Another concern is why this phenomenon and the Weddell Sea anomaly occur in the
4 southern summer. It is not clear from these data, but it may relate to the illumination of
5 the ionosphere as night is falling. The longitudinal extent of this phenomenon is also very
6 limited. It seems to be connected to the southward excursion of the magnetic equator. But
7 it does not occur at the longitude of the southernmost excursion of the magnetic equator;
8 instead it occurs on the western side of this bulge. There is no obvious reason why this
9 area should be favored over others, but its location and the formation of the Weddell Sea
10 anomaly in the same place for 50 years suggests that it is significant.

11 If we accept that this displacement is real, can we find a cause for it? The data provide a
12 number of features that must be reconciled by any explanation of this displacement. First,
13 the changes occur at dusk in a particular longitude sector. Second, they are associated
14 with a region in which the magnetic field moves far further south of the geographic
15 equator than it does anywhere else on the globe. Third, the displacement from the low
16 latitudes to the high latitudes is very fast. Fourth, there is a large hmF_2 increase on the
17 equatorward edge of the region of enhanced NmF_2 .

18 One way to change the height of the F_2 peak is through thermal expansion. As neutral
19 temperatures increase the atmosphere swells. The height of the F_2 peak tends to remain
20 on a constant pressure level (*Rishbeth and Edwards, 1989, 1990*), so it also increases.
21 However thermal expansion cannot explain what is seen in this paper for a number of
22 reasons. First, there is no increase in electron density associated with thermal expansion.
23 Second temperatures are expected to decrease from about 1500 LT (e.g., see *Mayr et al.*,

1 1978), so the atmosphere is contracting rather than expanding. Third, there is no known
2 reason why thermal expansion could possibly cause the latitude at which the electron
3 densities peak to change suddenly.

4 Other possible causes for the observed changes can be obtained from the O^+ continuity
5 equation (e.g., see *Burns et al.*, 2007). One possible mechanism is a change in neutral
6 composition. If the proportion of the heavy molecular gases in a column of air is
7 increased then the F_2 peak will move upwards. However, the recombination rate for O^+
8 also increases in this scenario leading to a decrease in electron densities at the F_2 peak.
9 Increases in O density compared with N_2 density can increase electron densities, but they
10 should move the F_2 peak downwards. So composition change does not seem to be a likely
11 explanation for the behavior seen in Figures 1 and 2.

12 Advection of ionization by the neutral winds provides another possible scenario.
13 Equatorward neutral winds blow up field lines, increasing the height of the F_2 peak and,
14 as this peak has moved to heights where there is less recombination, increasing electron
15 densities at the F_2 peak (e.g., *Prölss*, 1980). However, neutral winds are primarily zonal
16 at dusk, where the observed displacement occurs (e.g., *Burns et al.*, 1995), and have a
17 fairly smooth morphology over a large area (*Wu et al.*, 1995). Zonal neutral winds are not
18 efficient at driving electrons up field lines (a little upward or downward motion can
19 happen because the geographic and geomagnetic poles are at different locations), and the
20 relatively smooth morphology of the neutral wind field in low and middle latitudes in
21 quiet times argues against the neutral winds producing a relatively local change in
22 electron density like the one reported here.

1 Two terms are left in the O^+ continuity equation that could explain this behavior: the
2 electric field and ambipolar diffusion. One of the issues in trying to determine a cause of
3 the odd behavior of the electron density in the South Pacific is the speed at which the
4 electron densities change. If we accept the data in Figure 3b as evidence, the position of
5 the equatorial anomaly has moved about 30 degrees in less than an hour. Any direct
6 movement of the electrons would have to be supersonic, which would produce a shock.
7 No such shock has been reported. Any mechanism involving electric fields would
8 probably involve an advective process, which makes it less likely.

9 The last possibility is that there is a change in the plasmasphere that leads to a change in
10 the downward ambipolar diffusion of electrons. Such diffusion would lead to an increase
11 in electron densities and an increase in the height of the F_2 peak, particularly at the
12 equatorward edge of the disturbed region. Again, however, there is no known change in
13 the plasmasphere at dusk that might lead to this behavior.

14 An effort was made to model this behavior using the Coupled Magnetosphere Ionosphere
15 Thermosphere model (*Wang et al.*, 2004; *Wiltberger et al.*, 2004), which includes
16 interactive electric fields, but not an interactive plasmaspheric module. No feature like
17 the one described over the South Pacific in this paper was found in the output from this
18 model. Other modeling efforts that were reported by *Burns et al.* (2008) indicated that the
19 modeled electron densities decayed more rapidly than those observed by ionosondes after
20 dark in summer, suggesting that something is missing near dusk in the models in summer.
21 The behavior described in this paper could possibly explain this model-data discrepancy.

22

23

1 **Conclusions**

2

3

4 COSMIC data were analyzed to study the diurnal variation of electron densities in the
5 northern (southern) winter (summer) during quiet to moderate geomagnetic conditions.

6 During the daylight hours the data behaved just as it had done in numerous previous
7 studies. Equatorial anomalies formed on either side of the magnetic equator centered at

8 about 20 degrees geomagnetic latitude. The heights of these peaks and their location
9 conformed to the aforementioned previous studies. An odd thing happened just after dusk,

10 however. The southern equatorial anomaly over the South Pacific Ocean appeared to be
11 displaced rapidly south to about 60° S. In tandem with this behavior the height of these

12 enhanced electron densities increased on their equatorward edge. There is no evidence of
13 problems in the analysis procedure or the data. Individual data points were plotted that

14 showed the same behavior, so the analysis procedures at this level were not suspect. The
15 value of the more basic analysis procedures is demonstrated by the data reproducing the

16 expected behavior of the F_2 peak ionosphere at other times and locations. It is difficult to
17 imagine an analysis procedure or an observation that would fail in only one location

18 consistently over a period of three months. Furthermore, the end result of this behavior is
19 to produce another anomaly that has been extensively described using data gathered from

20 other, different observations.

21 While some causal mechanisms can be eliminated, no known physical mechanism

22 appears to explain the observed behavior. Thus, the COSMIC observations suggest that a

1 phenomenon is occurring over the South Pacific in the southern summer that we cannot,
2 at present, explain.

3

4

5 **Acknowledgements**

6

7 This research was supported by the Center for Integrated Space Weather Modeling (CISM) which is
8 funded by the STC program under agreement number ATM-0120950. NCAR is supported by the
9 National Science Foundation.

10

11

12 **References**

13

14

15 Beers, T. C., K. Flynn, and K. Gebhardt (1990), Measures of location and scale for
16 velocities in clusters of galaxies – a robust approach, *Astronom. J.*, 100(1), 32-46.

17 Bellchambers, W. H. and W. R. Piggott, Ionospheric measurements made at Halley Bay,
18 *Nature*, 188, 1596-1597, 1958

19 Bilitza, D. International Reference Ionosphere 2007, National Space Science Data Center,
20 <http://modelweb.gsfc.nasa.gov/ionos/iri.html> , Greenbelt, Maryland, 2007.

21 Burns, A. G., T. L. Killeen, W. Deng, G. R. Carignan, and R. G. Roble, Geomagnetic
22 storm effects in the low- and middle-latitude upper thermosphere, *J. Geophys. Res.*,
23 100, 14673-14691, 1995.

1 Burns, A. G., S. C. Solomon, W. Wang and T.L. Killeen, The ionospheric and
2 thermospheric response to CMEs: challenges and successes, *J. Atmos. Sol.-Terr.*
3 *Phys.*, 69, 77, 2007.

4 Burns A. G, W. Wang, M. Wiltberger, S. C. Solomon, H. Spence, T. L. Killeen, R. E.
5 Lopez, and J. E. Landivar, An event study to provide validation of TING and CMIT
6 geomagnetic middle latitude electron densities at the F₂ peak, in press *J. Geophys.*
7 *Res.*, 2008

8 Dudeney J. R. and W. R. Piggott, Antarctic ionospheric research, in *Upper Atmosphere*
9 *Research in Antarctica*, *Ant. Res. Ser.*, edited by L. J. Lanzerotti and C. G. Park, pp
10 200-235, Washington, D. C.

11 Hajj, G. A., and L. J. Romans, Ionospheric electron density profiles obtained with the
12 Global Positioning System: Results from the GPS/MET experiment, *Radio Sci.*, 33,
13 175–190. 1998

14 Horvath, I, A total electron content space weather study of the nighttime Weddell Sea
15 Anomaly of 1996/1997 southern summer with TOPEX/Poseidon radar altimetry, *J.*
16 *Geophys. Res.*, 111, A12317, doi:10.1029/2006JA011679, 2006.

17 Jee G., A. G. Burns, W. Wang, S. C. Solomon, R. W. Schunk, L. Scherliess, D. C.
18 Thompson, J. J. Sojka, L. Zhu, Duration of an ionospheric data assimilation
19 initialization of a coupled thermosphere-ionosphere model, *Space Weather*, 5, S01004,
20 doi:10.1029/2006SW000250, 2007.

21 Killeen, T. L. and R. G. Roble, Thermosphere Dynamics driven by magnetospheric
22 sources: contributions from the first five years of the Dynamics Explorer program,
23 *Rev. Geophys. Space Phys.*, 26 (2): 329-367, 1988.

1 Lei, J., S. Syndergaard, A. G. Burns, S. C. Solomon, W. Wang, Z. Zeng, R. G. Roble, Q.
2 Wu, Y.-H. Kuo, J. M Holt, S.-R. Zhang, D. L. Hysell, F. S. Rodrigues, and C. H. Lin,
3 Comparison of COSMIC ionospheric measurements with ground based observations
4 and model predictions: preliminary results, *J. Geophys. Res.*, 112, A07308,
5 doi:10.1029/2006JA012240, 2007

6 Kumar, M. (2006), New satellite constellation uses radio occultation to monitor space
7 weather, *Space Weather*, 4, S05003, doi:10.1029/2006SW000247.

8 Mayr, H. G., I. Harris, and N. W. Spencer, Some properties of upper-atmosphere
9 dynamics, *Rev. Geophys. Space Phys.*, 16, 539-565, 1978

10 Penndorf, R., The average ionospheric conditions over the Antarctic, in *Geomagnetism*
11 and *Aeronomy*, *Ant. Res. Ser.*, vol 4, edited by A. H. Waynick, pp1-45, AGU,
12 Washington, D. C.

13 Prölss, G. W., Magnetic storm associated perturbation of the upper atmosphere: recent
14 results obtained by satellite-borne gas analyzers, *Rev. Geophys. Space Phys.*, 18, 183-
15 202, 1980.

16 Rishbeth, H. and R. Edwards, The isobaric F₂-layer, *J. Atmos. Terr. Phys.*, 51, 321-338,
17 1989.

18 Rishbeth, H. and R. Edwards, Modeling the F₂ layer peak height in terms of atmospheric
19 pressure, *Radio Science*, 25, 757-769, 1990.

20 Rishbeth, H. and Garriott, O.K., 1969. *Introduction to ionospheric Physics*, Academic
21 Press, New York.

22 Rocken, C., Y.-H. Kuo, W. Schreiner, D. Hunt, S. Sokolovskiy, and C. McCormick, COSMIC system
23 description, *Terr. Atmos. Ocean Sci.*, 11, 21-52, 2000.

1 Schreiner, W. S., S. V. Sokolovskiy, C. Rocken, and D. C. Hunt (1999), Analysis and
2 validation of GPS/MET radio occultation data in the ionosphere, *Radio Sci.*, 34(4),
3 949-966.

4 Wang, W., M. Wiltberger, A. G. Burns, S. Solomon, T. L. Killeen, N. Maruyama, and J.
5 Lyon, Initial results from the CISM coupled magnetosphere-ionosphere-thermosphere
6 (CMIT) model: thermosphere ionosphere responses, *J. Atmos. Sol.-Terr. Phys.*, 66,
7 1425-1442, 2004.

8 Wiltberger, M., W. Wang, A. Burns, S. Solomon, J. G. Lyon, and C. C. Goodrich, Initial
9 results from the coupled magnetosphere ionosphere thermosphere model:
10 magnetospheric and ionospheric responses, *J. Atmos. Sol.-Terr. Phys.*, 66, 1411-1444
11 2004.

12 Wu, Q., T. L. Killeen, and N. W. Spencer, Dynamics Explorer 2 Observations of
13 Equatorial Thermospheric Winds and Temperatures: Local Time and Longitudinal
14 Dependences, *J. Geophys. Res.*, 99, 6277–6288, 1994.

15 Zeng, Z., A. G. Burns, W. Wang, J. Lei, S. C. Solomon, S. Syndergaard, L. Qian, and Y.-
16 H. Kuo, Ionospheric annual asymmetry observed by the COSMIC radio occultation
17 measurements and simulated by the TIEGCM, in press, *J. Geophys. Res.*, 2008
18
19

1 **Figures**

2

3 Figure 1. Global maps of NmF_2 calculated from COSMIC data for four local time bands:
4 a) 1700-1800 local time; b) 1800-1900 local time; c) 1900-2000 local time; d) 2000-2100
5 local time.

6

7 Figure 2. Global maps of hmF_2 calculated from COSMIC data for four local time bands:
8 a) 1700-1800 local time; b) 1800-1900 local time; c) 1900-2000 local time; d) 2000-2100
9 local time.

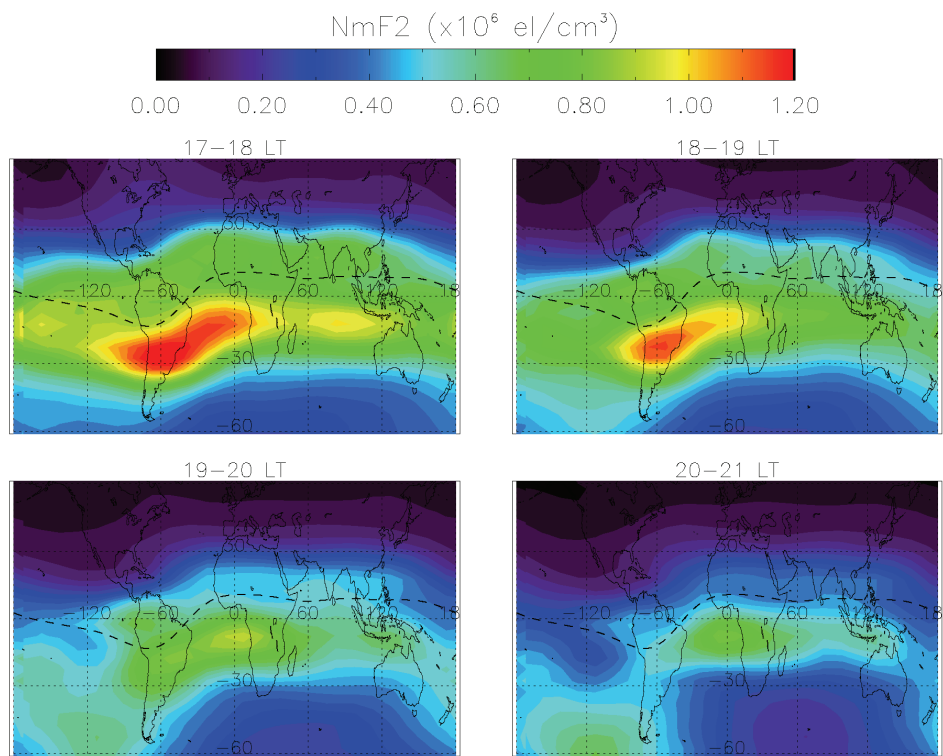
10

11 Figure 3. Individual data points of NmF_2 from COSMIC satellites for the 2000-2100 local
12 time bin

13

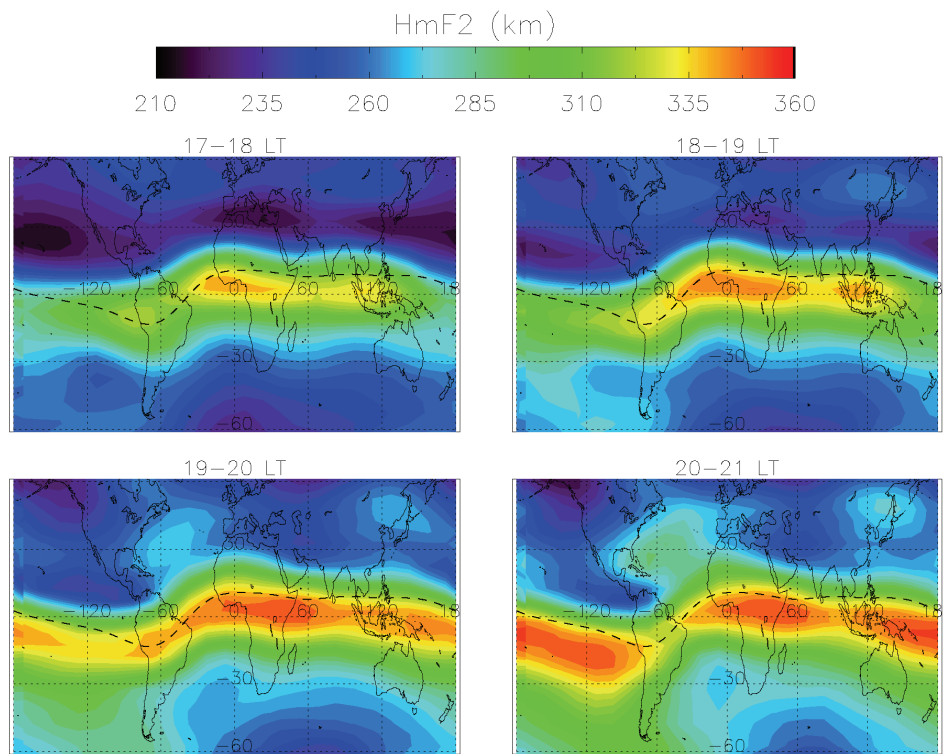
14

15



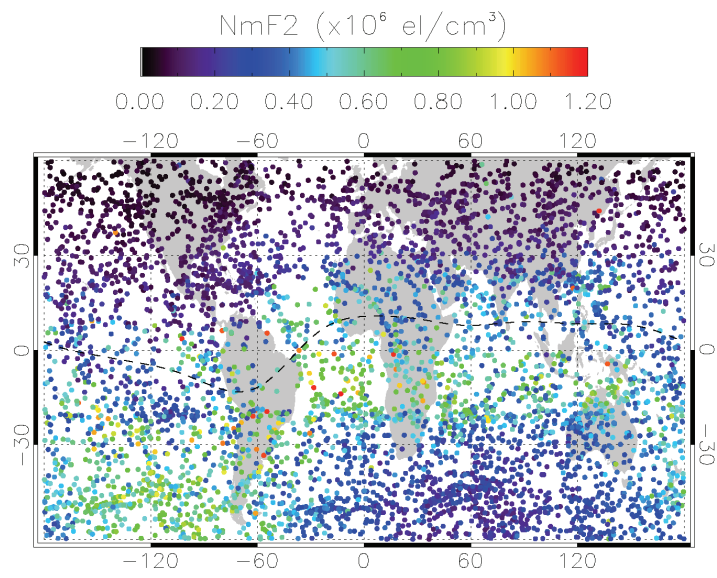
1

2 Figure 1



1

2 Figure 2



1

2 Figure 3

1

2